

Thermodynamics and phase transitions of a Kerr-Newman black hole in a cavity

Yuchen Huang^{a,b,*}, Jun Tao^{a,†}, Peng Wang^{a,‡} and Shuxuan Ying^{c,§}

^a*Center for Theoretical Physics, College of Physics,
Sichuan University, Chengdu, 610065, China*

^b*Department of Astronomy, School of Physical Sciences,
University of Science and Technology of China, Hefei, 230026, China and*

^c*Department of Physics, Chongqing University, Chongqing, 401331, China*

Abstract

The quasi-local energy of a Kerr-Newman black hole in a finite spherical cavity with fixed radius is derived from the Hamiltonian, and the first law of thermodynamics is constructed accordingly. In a canonical ensemble, the black hole could undergo a van der Waals-like phase transition. The temperature where the phase transition occurs decreases with the increase of the angular momentum or the charge. Our results imply that the thermodynamics of a Kerr-Newman black hole in a cavity shows extensive similarities to the one in AdS spacetime.

*Electronic address: huangyuchen@stu.scu.edu.cn

†Electronic address: taojun@scu.edu.cn

‡Electronic address: pengw@scu.edu.cn

§Electronic address: ysxuan@cqu.edu.cn

I. INTRODUCTION

One of the most appealing ways to define the energy of the gravitational field in a spatially bounded region follows from Brown and York's method [1]. In their pioneering work, the quasi-local energy is defined through the Hamiltonian. By means of such a definition, thermodynamic quantities for some simple gravitational systems enclosed by a cavity were obtained [2]. Nevertheless, there are several available reference backgrounds to choose. In many cases, the flat spacetime background is a preferred choice since it has the vanishing Hamiltonian. With this choice, the thermodynamics of a asymptotic flat Schwarzschild black hole enclosed by a spherical cavity was investigated in [3], where a phase transition that occurs between thermal flat spacetime and the black hole was found to be very similar to that of the Hawking-Page in AdS space [4]. Afterwards, the thermodynamics and phase transitions of a RN black hole in a cavity were studied in a grand canonical ensemble [5] and a canonical ensemble [6, 7], which exhibit some similarities to the black hole in asymptotic AdS space.

Recently, some works have been focusing on the thermodynamics of other types of black holes in a cavity, which devoted to comparing phase transitions of black holes under different boundary conditions, i.e., AdS space and the cavity. For example, a Born-Infeld black hole in a cavity [8, 9], a Gauss-Bonnet black hole in a cavity [10], a RN black hole surrounded by quintessence in a cavity [11], a spontaneously scalarized RN black hole in a cavity [12] and a BTZ black hole in a cavity [13] were fully studied. The main conclusion is that the thermodynamics and phase transitions of black holes under the two different boundary conditions show close resemblances but several dissimilarities. Furthermore, the thermodynamics of a black hole in a cavity can be discussed in an extended phase space, where the volume of the cavity was treated as a thermodynamic volume [14]. Other thermodynamic properties for black holes in a cavity such as the Ruppeiner geometry were also investigated in [15, 16], which indicated that there may be a connection between black hole microstates and boundary conditions [15]. On the whole, most discussions about the thermodynamics of black holes in a cavity especially phase transitions, were based on static black holes. Although the rotating BTZ black hole was discussed in [13], it did not show rich phase structures due to the non-negative heat capacity. Therefore, one naturally generalizes the study to a rotating and charged Kerr-Newman black hole.

The Kerr-Newman metric is an exact solution of the Einstein-Maxwell equation, which describes stationary spacetime with the angular momentum and the electric charge. In 1963, Kerr first found the metric of a spinning object in a gravitational field [17], which is a generalization of the Schwarzschild metric. Two years later, Newman et al. obtained the metric that can describe both rotating and charged spacetime [18]. Later on, with the advent of AdS/CFT conjecture [19, 20], the thermodynamics of a Kerr-Newman black hole in AdS space was studied in [21], where the Hawking-Page phase transition was found in a grand canonical ensemble, and a van de Waals-like phase transition was found in a canonical ensemble. Other thermodynamic properties of the Kerr-Newman black hole under different conditions were extensively studied [22–29]. It was proposed by Smarr that under some specific conditions, the two-dimensional hypersurface of the Kerr spacetime can not be globally embedded in the three-dimensional Euclidean space [30], therefore only the quasi-local energy with a small angular momentum of the Kerr black hole was obtained [31]. A counterterm prescription inspired by the AdS/CFT conjecture was proposed [32–35], which solved this issue and was used to calculate the quasi-local energy and thermodynamic quantities of the Kerr and Kerr-AdS black holes [36]. After that, the quasi-local energy and thermodynamic quantities of the Kerr-dS and Kerr-Newman-dS black holes were also investigated in [37, 38]. Nevertheless, rotating and charged black holes in a cavity still remain some unknowns at the phase transition level.

In this work, we probe the thermodynamics and phase transitions of a Kerr-Newman black hole in a cavity. The quasi-local energy we adopt is defined by the Brown-York method. To make the Hamiltonian well defined, a counterterm prescription is considered. The following part of this paper is organized as follows: In section II, we derive the quasi-local energy for the Kerr-Newman black hole and construct the first law of thermodynamics. In section III, we study the phase transition in a canonical ensemble and plot phase diagrams. The closing remarks are presented in section IV.

II. QUASI-LOCAL ENERGY AND THERMODYNAMICS

We start from the volume gravitational action coupled to the electromagnetic field,

$$\mathcal{S}_v = \frac{1}{16\pi} \int_{\mathcal{M}} d^4x \sqrt{-g} (R - F^{\mu\nu} F_{\mu\nu}), \quad (1)$$

where R is the Ricci scalar of the manifold \mathcal{M} , and $F_{\mu\nu} = \partial_\mu A_\nu - \partial_\nu A_\mu$ is the electromagnetic field tensor. To give the correct field equation, a boundary term is required, and it is given by

$$\mathcal{S}_b = \frac{1}{8\pi} \int_{\partial\mathcal{M}} d^3x \varepsilon \sqrt{|h|} K. \quad (2)$$

The integral of the above formula is calculated on the boundary $\partial\mathcal{M}$, which can be written as the union of three parts $\partial\mathcal{M} = (-\Sigma_{t'}) \cup \Sigma_{t''} \cup \mathcal{B}$, where $\Sigma_{t'}$, $\Sigma_{t''}$ are two spacelike boundaries, and \mathcal{B} is a timelike boundary. Besides, K is the trace of the extrinsic curvature on $\partial\mathcal{M}$ as embedded in \mathcal{M} , and $\varepsilon = 1$ if $\partial\mathcal{M}$ is timelike while $\varepsilon = -1$ if $\partial\mathcal{M}$ is spacelike. The foliation of the manifold is presented in FIG. 1. It turns out that the value of the action is divergent if one extends the boundary to infinity. Therefore, an extra term is needed to eliminate this divergence. Although this term is not always uniquely determined [39], a natural choice is

$$\mathcal{S}_0 = -\frac{1}{8\pi} \int_{\partial\mathcal{M}} d^3x \varepsilon \sqrt{|h|} K_0, \quad (3)$$

where K_0 is the extrinsic curvature of $\partial\mathcal{M}$ that embedded in flat spacetime. This term makes the value of the action vanish when spacetime is flat. For a Kerr spacetime, not all the two-boundary surfaces are possible to be globally embedded in three-dimensional Euclidean space [30], which makes the extra term not well defined, and hence only the quasi-local energy with a small angular momentum is obtained [31]. To address these difficulties, one can resort to a counterterm prescription, which suggests that the term \mathcal{S}_0 in Eq. (3) should be replaced by [32–34]

$$\mathcal{S}_{ct} = -\frac{1}{8\pi} \int_{\partial\mathcal{M}} d^3x \varepsilon \sqrt{|h|} \sqrt{2\mathcal{R}}, \quad (4)$$

where \mathcal{R} denotes the Ricci scalar on the three-boundary \mathcal{B} . Some analyses focus on another similar counterterm that substitutes \mathcal{R} with the Ricci scalar of the two-boundary \mathcal{B} , which is also called a lightcone reference [35]. In the following part, we will calculate thermodynamic quantities mainly based on the counterterm in Eq. (4) and make a brief discussion in the closing remark section about the thermodynamics in the lightcone reference. The geometric quantities in this paper are shown in TABLE I.

To obtain the Hamiltonian, one performs a (3 + 1) decomposition on the manifold \mathcal{M} and arrives at [40]

$$\mathcal{S} = \frac{1}{16\pi} \int_{t'}^{t''} dt \left[\int_{\Sigma_t} d^3x (\mathcal{R} + K^{ab} K_{ab} - K^2 - F^{\mu\nu} F_{\mu\nu}) N \sqrt{h} + 2 \int_{\mathcal{B}} d^2x \left(k - \sqrt{2\mathcal{R}} \right) N \sqrt{\sigma} \right], \quad (5)$$

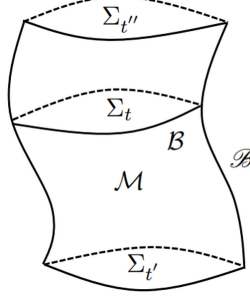


FIG. 1: Manifold \mathcal{M} and its foliation. The boundary $\partial\mathcal{M} = (-\Sigma_{t'}) \cup \Sigma_{t''} \cup \mathcal{B}$. The boundary of the spacelike hypersurface Σ_t that embedded in \mathcal{M} is \mathcal{B} .

| Manifold | Metric | Covariant Derivative | Curvature | Extrinsic Curvature | Unit Normal | Tangent Vector |
|---------------|-------------------|----------------------|-----------------|---------------------|-------------|----------------|
| \mathcal{M} | $g_{\alpha\beta}$ | $;\alpha$ | R | | | |
| Σ_t | h_{ab} | $ _a$ | \mathcal{R} | K_{ab} | n_α | e_a^α |
| \mathcal{B} | γ_{ij} | | \mathcal{R} | \mathcal{K}_{ij} | r_α | e_i^α |
| \mathcal{B} | σ_{AB} | | \mathcal{R}_L | k_{AB} | r_a | e_A^α |

TABLE I: Geometric quantities in this paper.

where Σ_t describes a constant time hypersurface, \mathcal{R} is the Ricci scalar on Σ_t , N is the lapse function, σ denotes the determinant of the metric of \mathcal{B} , and k is the trace of the extrinsic curvature of \mathcal{B} as embedded in Σ_t . Regarding h_{ab} as the dynamic variable of the gravitational field, one obtains the corresponding conjugated momentum [40]

$$p^{ab} = \frac{\partial(\sqrt{-g}\mathcal{L}_G)}{\partial\dot{h}_{ab}} = \frac{1}{16\pi}\sqrt{h}(K^{ab} - Kh^{ab}), \quad (6)$$

where \mathcal{L}_G is the Lagrangian of the pure gravitational field. The dot over h_{ab} denotes the Lie derivative along $t^\alpha = Nn^\alpha + N^ae_a^\alpha$, where N^a is the shift function. The dynamic variable of the pure electromagnetic field is $\partial_0 A_a$, and hence the conjugated momentum is

$$\mathcal{P}^a = -\frac{\sqrt{-g}}{16\pi} \frac{\partial(F^{\mu\nu}F_{\mu\nu})}{\partial(\partial_0 A_a)} = -\frac{\sqrt{-g}}{4\pi} F^{0a}. \quad (7)$$

Consequently, the Hamiltonian density can be written as

$$\mathcal{H} = p^{ab}\dot{h}_{ab} + \mathcal{P}^a\partial_0 A_a - \sqrt{-g}(\mathcal{L}_G - F^{\mu\nu}F_{\mu\nu}). \quad (8)$$

The Hamiltonian of the system can be obtained by integrating the Hamiltonian density in

the space region Σ_t and adding the boundary term,

$$H = \frac{1}{16\pi} \int_{\Sigma_t} d^3x \sqrt{h} (NC - 2N_a \mathcal{C}^a + A_0 \mathcal{G}) - \frac{1}{8\pi} \int_{\mathcal{B}} d^2x \sqrt{\sigma} \left[N \left(k - \sqrt{2\mathcal{R}} \right) - N_a (K^{ab} - Kh^{ab}) r_b - \frac{8\pi}{\sqrt{h}} A_0 r_a \mathcal{P}^a \right], \quad (9)$$

where r_a is the unit normal of \mathcal{B} as embedded in Σ_t . Furthermore, we have three constraint equations. The Hamiltonian constraint reads

$$\mathcal{C} = K^{ab} K_{ab} - K^2 - \mathcal{R} + 16\pi\rho = 0, \quad (10)$$

where $\rho = T_{\alpha\beta} n^\alpha n^\beta$ is the energy density of the electromagnetic field, and $T_{\alpha\beta}$ denotes the energy-momentum tensor,

$$T^{\alpha\beta} = \frac{1}{4\pi} g_{\mu\nu} F^{\alpha\mu} F^{\beta\nu} - \frac{1}{16\pi} g^{\alpha\beta} F^{\mu\nu} F_{\mu\nu}. \quad (11)$$

The momentum constraint reads

$$\mathcal{C}^a = (K^{ab} - Kh^{ab})|_b - 8\pi j^a = 0, \quad (12)$$

where $j_a = T_{\alpha\beta} e_a^\alpha n^\beta$ is the momentum density of the field. The Gauss's-law constraint reads

$$\mathcal{G} = -\frac{16\pi}{\sqrt{h}} \mathcal{P}^a{}_{,a} = 0. \quad (13)$$

With these three constraint equations, the Hamiltonian reduces to

$$H = -\frac{1}{8\pi} \int_{\mathcal{B}} d^2x \sqrt{\sigma} \left[N \left(k - \sqrt{2\mathcal{R}} \right) - N_a (K^{ab} - Kh^{ab}) r_b - \frac{8\pi}{\sqrt{h}} A_0 r_a \mathcal{P}^a \right]. \quad (14)$$

The mass-energy of the gravitational system inside the boundary \mathcal{B} is defined as the first term in the Hamiltonian (14) with the choice of lapse $N = 1$ [1, 41],

$$E = -\frac{1}{8\pi} \int_{\mathcal{B}} d^2x \sqrt{\sigma} \left(k - \sqrt{2\mathcal{R}} \right), \quad (15)$$

which will be regarded as the thermodynamic internal energy.

We consider the Kerr-Newman spacetime, whose metric in the Boyer-Lindquist-type coordinates is given by [18, 40]

$$ds^2 = -\frac{\Delta}{\rho^2} (dt - a \sin^2 \theta d\phi)^2 + \frac{\rho^2}{\Delta} dr^2 + \rho^2 d\theta^2 + \frac{\sin^2 \theta}{\rho^2} \left[a dt - (r^2 + a^2) d\phi \right]^2, \quad (16)$$

$$A_\alpha dx^\alpha = -\frac{Qr}{\rho^2} (dt - a \sin^2 \theta d\phi),$$

with

$$\begin{aligned}\rho^2 &= r^2 + a^2 \cos^2 \theta, \\ \Delta &= r^2 - 2Mr + a^2 + Q^2,\end{aligned}\tag{17}$$

where M is the ADM mass, $a = J/M$ is the magnitude of the angular momentum per unit mass, and Q is the charge. The event horizon radius r_+ is determined by a coordinate singularity $\Delta = 0$, i.e., $r_+^2 - 2Mr_+ + a^2 + Q^2 = 0$. The induced line element on the constant time hypersurface Σ_t can be written as

$$ds^2|_{\Sigma_t} = \frac{\rho^2}{\Delta} dr^2 + \rho^2 d\theta^2 + \frac{\sin^2 \theta}{\rho^2} \left[(r^2 + a^2)^2 - a^2 \Delta \sin^2 \theta \right] d\phi^2.\tag{18}$$

We consider the system that the black hole is enclosed by a cavity with a fixed radius r_B .

The line element on the hypersurface \mathcal{B} thus is given by

$$ds^2|_{\mathcal{B}} = (r_B^2 + a^2 \cos^2 \theta) d\theta^2 + \frac{\sin^2 \theta}{r_B^2 + a^2 \cos^2 \theta} \left[(r_B^2 + a^2)^2 - a^2 (r_B^2 - 2Mr_B + a^2 + Q^2) \sin^2 \theta \right] d\phi^2.\tag{19}$$

The determinant of the metric of \mathcal{B} can be extracted from the line element above,

$$\sigma = a^4 \sin^2 \theta \cos^2 \theta + 2a^2 m r_B \sin^4 \theta - a^2 Q^2 \sin^4 \theta - a^2 r_B^2 \sin^4 \theta + 2a^2 r_B^2 \sin^2 \theta + r_B^4 \sin^2 \theta.\tag{20}$$

The trace of the extrinsic curvature k_{ab} of \mathcal{B} that embedded in Σ_t is

$$k = r^a|_a = \frac{a^2 \sin^2 \theta (r_B - M) - 2r_B (a^2 + r_B^2)}{a^2 \sin^2 \theta (a^2 - 2Mr_B + Q^2 + r_B^2) - (a^2 + r_B^2)^2} \times \left(\frac{a^2 - 2Mr_B + Q^2 + r_B^2}{a^2 \cos^2 \theta + r_B^2} \right)^{1/2}.\tag{21}$$

The Ricci scalar of the boundary \mathcal{B} with a fixed radius arrives at

$$\mathcal{R} = \frac{2r_B^4 + 2a^2 (r_B^2 - 2Mr_B + Q^2) \cos^2 \theta}{(r_B^2 + a^2 \cos^2 \theta)^3}.\tag{22}$$

With these preliminaries, we then calculate the energy of the black hole in a cavity. A straightforward calculation of Eq. (15) gives

$$E = \int_0^\pi d\theta E_\theta (a, M, r_B, Q, \theta),\tag{23}$$

where

$$\begin{aligned}E_\theta (a, M, r_B, Q, \theta) &= \left[(a^2 + r_B^2)^2 \sin^2 \theta - a^2 \sin^4 \theta (a^2 - 2Mr_B + Q^2 + r_B^2) \right]^{1/2} \\ &\times \left\{ \frac{2a^2 \cos^2 \theta (r_B^2 + Q^2 - 2Mr_B) + 2r_B^4}{(2a^2 \cos^2 \theta + 2r_B^2)^3} \right\}^{1/2} \\ &+ \frac{a^2 \sin^4 \theta (r_B - M) - 2r_B (a^2 + r_B^2) \sin^2 \theta}{4 \left[(a^2 + r_B^2)^2 \sin^2 \theta - a^2 \sin^4 \theta (a^2 - 2Mr_B + Q^2 + r_B^2) \right]^{1/2}} \times \left(\frac{a^2 - 2Mr_B + Q^2 + r_B^2}{a^2 \cos^2 \theta + r_B^2} \right)^{1/2}.\end{aligned}\tag{24}$$

Extending the cavity radius to infinity, we can obtain the ADM mass,

$$\lim_{r_B \rightarrow \infty} E = M. \quad (25)$$

Moreover, when the angular momentum vanishes, the energy reduces to

$$E = r_B \left(1 - \sqrt{1 - \frac{2M}{r_B} + \frac{Q^2}{r_B^2}} \right), \quad (26)$$

which is the energy of a RN black hole in a cavity [5]. The entropy of the Kerr-Newman black hole equals to one quarter of the event horizon area,

$$S = \frac{1}{4}A = \pi (r_+^2 + a^2). \quad (27)$$

We consider the following three equations: the event horizon determined by $\Delta = 0$ in Eq. (17), the angular momentum $J = Ma$ and the entropy in Eq. (27). Solving these equations, one obtains the rotating parameter a and the ADM mass M as functions of the entropy, the angular momentum and the charge: $a(S, J, Q)$ and $M(S, J, Q)$. After inserting functions $a(S, J, Q)$ and $M(S, J, Q)$ into $E(a, M, r_B, Q)$ in Eq. (23), we rewrite the energy as $E(S, J, Q, r_B)$. We then define the temperature as the derivative of the energy with respect to the entropy while keeping J, Q, r_B fixed,

$$T(S, J, Q, r_B) = \left(\frac{\partial E}{\partial S} \right)_{J, Q, r_B} = \int_0^\pi d\theta \left(\frac{\partial E_\theta}{\partial S} \right)_{J, Q, r_B}. \quad (28)$$

In the second equality, we have swapped the order of the derivative and the integral. Similarly, the angular velocity and the electric potential are defined as

$$\begin{aligned} \Omega(S, J, Q, r_B) &= \int_0^\pi d\theta \left(\frac{\partial E_\theta}{\partial J} \right)_{S, Q, r_B}, \\ \Phi(S, J, Q, r_B) &= \int_0^\pi d\theta \left(\frac{\partial E_\theta}{\partial Q} \right)_{S, J, r_B}. \end{aligned} \quad (29)$$

Therefore, the first law of thermodynamics can be written as

$$dE = TdS + \Omega dJ + \Phi dQ. \quad (30)$$

Without loss of generality, we set the cavity radius $r_B = 1$ and keep it invariant in the following discussions to simplify the calculation.

III. PHASE TRANSITION

We first analyze the thermodynamic stability of the black hole in a canonical ensemble by considering the heat capacity at fixed angular momentum and the charge,

$$C_{J,Q} = T \left(\frac{\partial S}{\partial T} \right)_{J,Q} = T / \left(\frac{\partial T}{\partial S} \right)_{J,Q}. \quad (31)$$

The sign of the heat capacity agrees with the sign of the derivative of the temperature with respect to the entropy. Due to the absence of an analytic expression, we resort to numerical methods to investigate the behavior of the heat capacity. Plots of the temperature with respect to the entropy are presented in FIG. 2. In the left panel, one fixes the angular momentum $J = 0.02$, and each curve corresponds to a unique value of the charge. When the charge is less than the critical value, we can divide the curve into three branches according to the slope, and it shows that there are three types of black holes for some range of temperatures (the temperature between a local minimum and a local maximum): small (stable) black holes, medium (unstable) black holes and large (stable) black holes, corresponding to branches with positive, negative and positive slopes, respectively. With the increase of the charge, the three types of black holes finally become one type of black hole, which is globally stable. The critical case appears when $Q = Q_c \approx 0.2120$, that is, the local maximum and minimum of the temperature coincide. In the right panel, we fix the charge $Q = 0.10$, and each curve possesses a unique value of the angular momentum. When the angular momentum is less than the critical value, there are also three branches for some range of temperatures, which correspond to small, medium and large black holes. The critical case appears when $J = J_c \approx 0.0377$. Only one single solution for the black hole exists when the angular momentum is greater than the critical value.

It turns out that our model is suitable when the cavity radius r_B is greater than the event horizon radius r_+ , therefore $r_+ < 1$. This can be used to constrain physical quantities of the black hole in a cavity. We turn to consider the three equations mentioned above: the horizon radius determined by $\Delta = 0$ in Eq. (17), the angular momentum $J = Ma$ and the entropy in Eq. (27). Solving these equations yields

$$r_+(S, J, Q) = \frac{\sqrt{S}(\pi Q^2 + S)}{\sqrt{\pi} \sqrt{4\pi^2 J^2 + (\pi Q^2 + S)^2}} < 1. \quad (32)$$

According to this inequality, we can plot the maximal value of the entropy in the angular

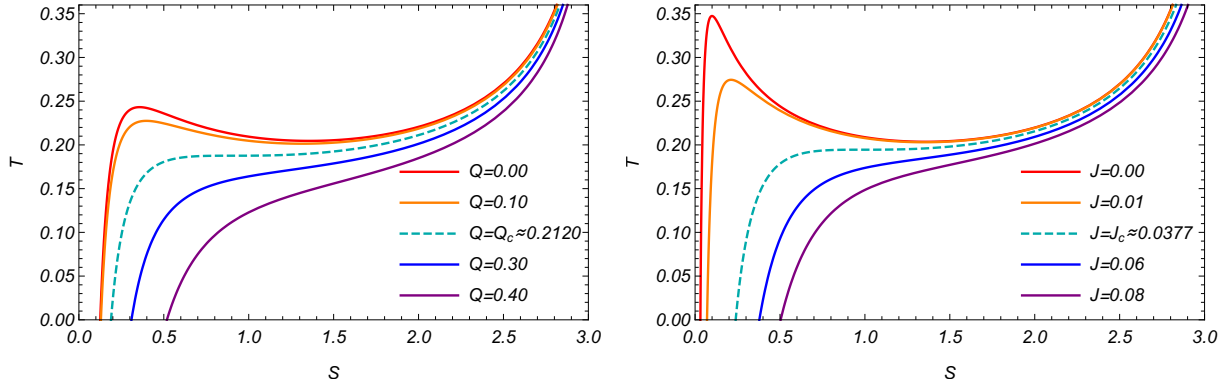


FIG. 2: Plots of the temperature with respect to the entropy with fixed angular momentum or charge. **Left Panel** The angular momentum $J = 0.02$. The charge $Q = Q_c \approx 0.2120$ corresponds to a critical curve. **Right Panel** The charge $Q = 0.10$. The angular momentum $J = J_c \approx 0.0377$ corresponds to a critical curve.

momentum-charge parameter space, which is exhibited in FIG. 3. It implies that when the angular momentum J is fixed, the maximal entropy decreases as the charge increases. When the charge is fixed, the maximal entropy increases as the angular momentum increases. Moreover, we can further probe all possible values of the angular momentum and the charge of the Kerr-Newman black hole in a cavity. The physically allowed region of the angular momentum and the charge in the parameter space is solved by numerical methods and shown in the right panel of FIG. 3. The region where a phase transition occurs is also outlined in the diagram, and it is situated inside the region where the black hole exists. We find this region shows striking resemblances to the one of the Kerr-Newman black hole in AdS space [21].

In a canonical ensemble, the angular momentum and the charge are fixed. Thus the Helmholtz free energy is used to investigate phase transitions. The Helmholtz free energy is defined as $F = E - TS$, which can also be written as a function of S , J and Q . We choose different values of angular momentum and charge and plot curves of the free energy against the temperature in FIG. 4. In the left column, the angular momentum $J = 0.02$, and the charge $Q = 0.10 < Q_c$, $Q = Q_c \approx 0.2120$, from top to bottom. When the charge is less than the critical value, there are three types of black holes at most: small, medium and large black holes. At a low temperature, there is only a small black hole, which is

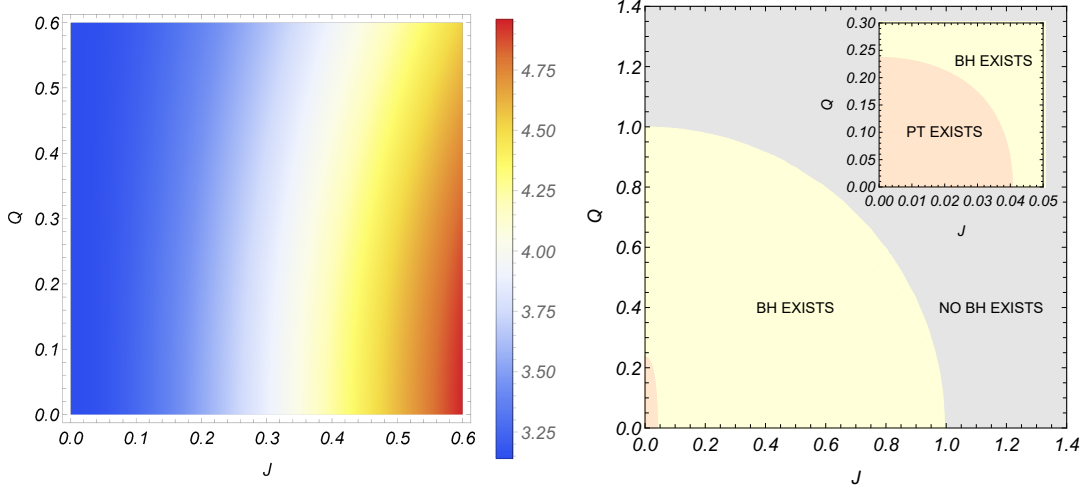


FIG. 3: **Left Panel** The maximal value of the entropy in the angular momentum-charge plane. **Right Panel** The physically allowed region and the region where a phase transition exists in the angular momentum-charge plane.

thermodynamically stable. As the temperature increases, the medium black hole and the large black hole appear, but the small black hole is still the stable state until the occurrence of a first-order phase transition. After the phase transition, the small black hole becomes a metastable state, and the large black hole becomes a stable state. When the charge increases to the critical value, i.e., $Q_c \approx 0.2120$, there are two types of black holes. The small black hole exists at a low temperature and transits into the large black hole at a high temperature through a second-order phase transition. As the charge increases further, there is only one type of black hole that is globally stable, and no phase transition occurs. In the right column, the charge $Q = 0.10$, and the angular momentum $J = 0.01 < J_c$, $J = J_c \approx 0.0377$, from top to bottom. When the angular momentum is less than the critical value, there are three types of black holes. As the temperature increases, a first-order phase transition occurs from the small black hole to the large black hole. When the angular momentum increases to the critical value, there are two types of black holes, and a second-order phase transition occurs between the small black hole and the large black hole. When the angular momentum is greater than the critical value, there is only one type of black hole.

Phase diagrams in temperature-charge and temperature-angular momentum planes are exhibited in FIG. 5. In the left panel, the angular momentum $J = 0.02$. A first-order phase

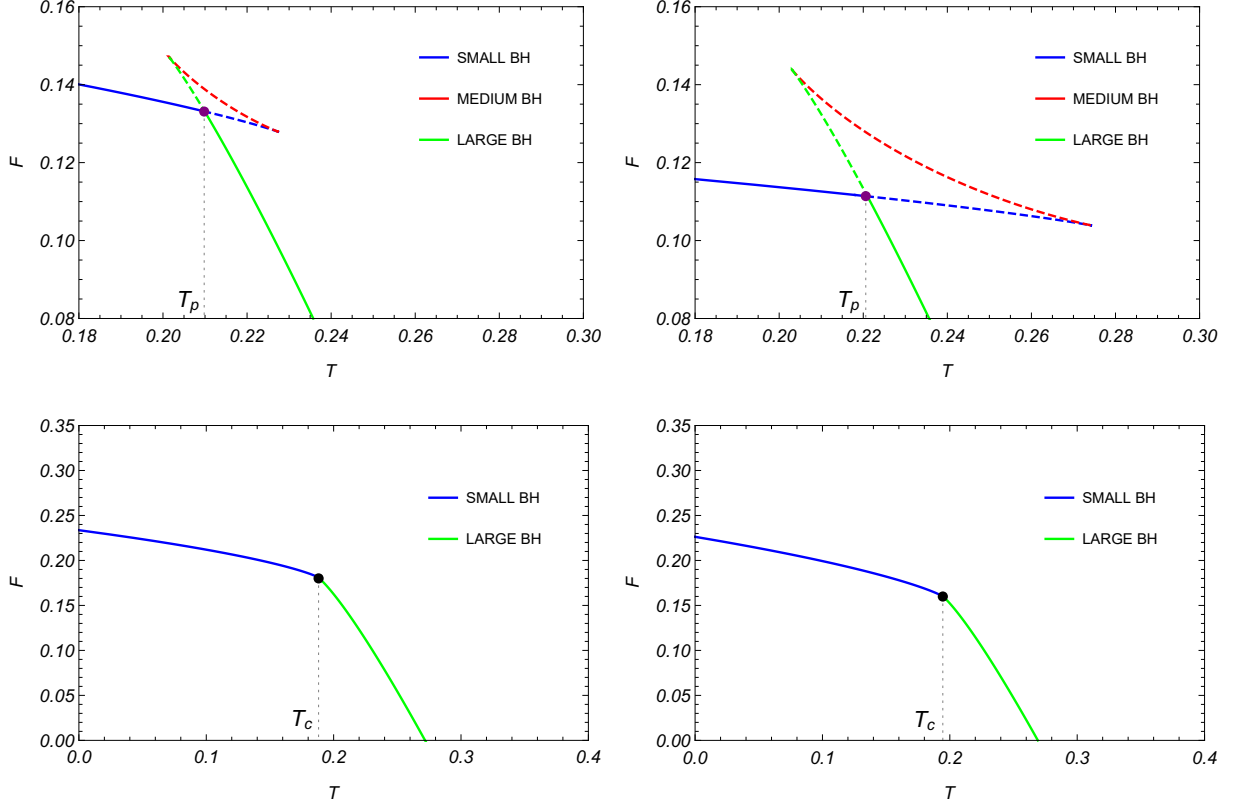


FIG. 4: Plots of the free energy with respect to the temperature. Dashed curves correspond to unstable or metastable states, and solid curves to stable states. First-order phase transitions occur on purple dots and second-order phase transitions occur on black dots. **Left Column** The angular momentum $J = 0.02$. The charge $Q = 0.10 < Q_c$, $Q = Q_c \approx 0.2120$ from top to bottom. **Right Column** The charge $Q = 0.10$. The angular momentum $J = 0.01 < J_c$, $J = J_c \approx 0.0377$ from top to bottom.

transition occurs on the purple curve. The small black hole is thermodynamically stable at the temperature lower than the purple curve, and the large black hole is thermodynamically stable in the region with the temperature higher than that of the purple curve. As the charge increases, the phase transition temperature decreases, and the first-order phase transition curve finally terminates at a critical point, where a second-order phase transition occurs. After the charge gets higher than the critical value, no phase transition occurs, and there is only a single phase. In the right panel, the charge $Q = 0.10$. The temperature where the first-order phase transition occurs decreases as the angular momentum increases. After the occurrence of a second-order phase transition, there is only a single phase, and no phase

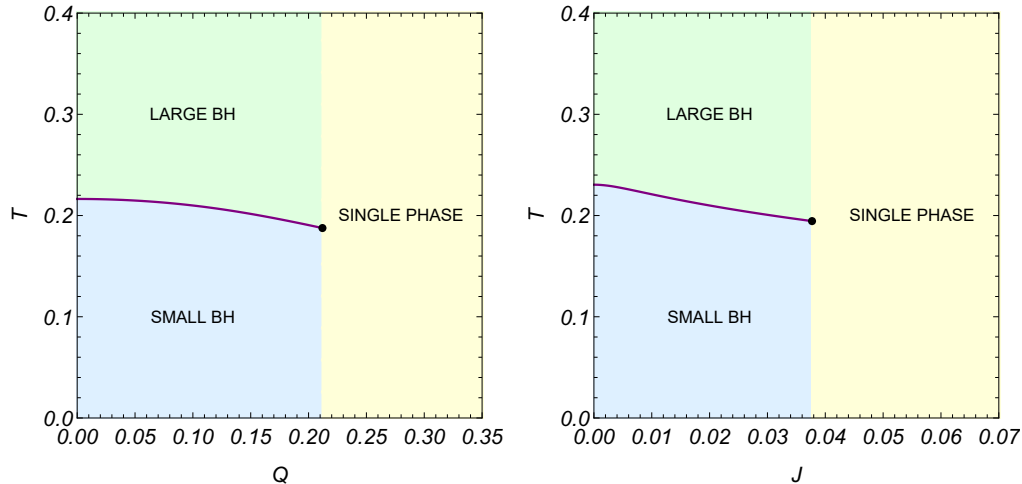


FIG. 5: Phase diagrams of the Kerr-Newman black hole in a cavity. First-order phase transitions occur on purple curves, and second-order phase transitions occur on black dots. Small black holes are globally stable in blue regions while large black holes are globally stable in green regions. **Left Panel** The angular momentum $J = 0.02$. **Right Panel** The charge $Q = 0.10$.

transition occurs.

IV. CLOSING REMARKS

The thermodynamics of a Kerr-Newman black hole in a cavity were investigated in this paper. We derived the quasi-local energy defined by the Hamiltonian and constructed the first law of thermodynamics accordingly. For the Kerr-Newman black hole in a cavity, there is an upper bound for the event horizon radius, which yields a constraint on the entropy, the angular momentum and the charge. The maximal value of entropy in the angular momentum-charge plane was then plotted in the left panel of FIG. 3. Based on this constraint, we further investigated all possible values for the angular momentum and the charge. The physically allowed region in the angular momentum-charge parameter space was presented in the right panel of FIG. 3. To study phase transitions of the black hole, we plotted the Helmholtz free energy with respect to the temperature with fixed angular momentum and charge in a canonical ensemble in FIG. 4. We found a first-order phase transition that occurs from the small black hole to the large black hole as the temperature increases, and it finally terminates at a critical point where a second-order phase transition

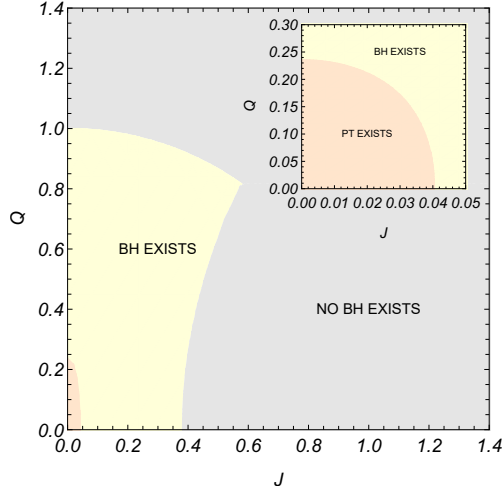


FIG. 6: The physically allowed region and the region where a phase transition exists in the angular momentum-charge plane in the lightcone reference.

occurs. It follows that the Kerr-Newman black hole in a cavity shows similar phase structures to the van der Waals fluid. Phase diagrams were presented in FIG. 5, where we found that the increase of the angular momentum or the charge will decrease the first-order phase transition temperature. The phase diagram with fixed angular momentum and the one with fixed charge show slight differences. It turns out that the phase structures of a Kerr-Newman black hole in a cavity and a Kerr-Newman-AdS black hole show extensive similarities.

Different from static black holes in a cavity, we found that the quasi-local energy of a Kerr-Newman black hole in a cavity depends on the background reference. More precisely, different counterterms in Eq. (4) will generate different results on quasi-local energy and thermodynamic quantities. One can also calculate the quasi-local energy in a lightcone reference. Therefore, a quantity ΔE can be used to characterize the difference between the quasi-local energy in our previous reference and the one in the lightcone reference,

$$\Delta E = \frac{1}{8\pi} \int_{\mathcal{B}} d^2x \sqrt{\sigma} \left(\sqrt{2\mathcal{R}} - \sqrt{2\mathcal{R}_L} \right), \quad (33)$$

where \mathcal{R}_L is the Ricci scalar on the two-boundary \mathcal{B} . It is straightforward to show that ΔE vanishes in two special cases: the angular momentum $J = 0$, and the cavity radius $r_B \rightarrow \infty$. Consequently, the difference of thermodynamics on both references only emerges in the rotating black hole in a cavity. Furthermore, we found the numerical difference between both references is small on the thermodynamics and phase transitions but significant in

the physically allowed region in the angular momentum-charge parameter space, as shown in FIG. 6. A detailed analysis also shows that, the difference between thermodynamic quantities of the two references increases as the angular momentum increases, and decreases as the charge increases.

V. ACKNOWLEDGMENTS

We are grateful to Yihe Cao, Qi Xu and Jiayi Wu for useful discussions and valuable comments. This work is supported by NSFC (Grant No.12147207 and 12105031).

-
- [1] J. David Brown and James W. York, Jr. Quasilocal energy and conserved charges derived from the gravitational action. *Phys. Rev. D*, 47:1407–1419, 1993. [arXiv:gr-qc/9209012](#), [doi:10.1103/PhysRevD.47.1407](#).
 - [2] J. David Brown, J. Creighton, and Robert B. Mann. Temperature, energy and heat capacity of asymptotically anti-de Sitter black holes. *Phys. Rev. D*, 50:6394–6403, 1994. [arXiv:gr-qc/9405007](#), [doi:10.1103/PhysRevD.50.6394](#).
 - [3] James W. York, Jr. Black hole thermodynamics and the Euclidean Einstein action. *Phys. Rev. D*, 33:2092–2099, 1986. [doi:10.1103/PhysRevD.33.2092](#).
 - [4] S. W. Hawking and Don N. Page. Thermodynamics of Black Holes in anti-De Sitter Space. *Commun. Math. Phys.*, 87:577, 1983. [doi:10.1007/BF01208266](#).
 - [5] Harry W. Braden, J. David Brown, Bernard F. Whiting, and James W. York, Jr. Charged black hole in a grand canonical ensemble. *Phys. Rev. D*, 42:3376–3385, 1990. [doi:10.1103/PhysRevD.42.3376](#).
 - [6] Steven Carlip and S. Vaidya. Phase transitions and critical behavior for charged black holes. *Class. Quant. Grav.*, 20:3827–3838, 2003. [arXiv:gr-qc/0306054](#), [doi:10.1088/0264-9381/20/16/319](#).
 - [7] Andrew P. Lundgren. Charged black hole in a canonical ensemble. *Phys. Rev. D*, 77:044014, 2008. [arXiv:gr-qc/0612119](#), [doi:10.1103/PhysRevD.77.044014](#).
 - [8] Peng Wang, Houwen Wu, and Haitang Yang. Thermodynamics and Phase Transition of a Nonlinear Electrodynamics Black Hole in a Cavity. *JHEP*, 07:002, 2019. [arXiv:1901.06216](#),

[doi:10.1007/JHEP07\(2019\)002](https://doi.org/10.1007/JHEP07(2019)002).

- [9] Kangkai Liang, Peng Wang, Houwen Wu, and Mingtao Yang. Phase structures and transitions of Born–Infeld black holes in a grand canonical ensemble. *Eur. Phys. J. C*, 80(3):187, 2020. [arXiv:1907.00799](https://arxiv.org/abs/1907.00799), [doi:10.1140/epjc/s10052-020-7750-z](https://doi.org/10.1140/epjc/s10052-020-7750-z).
- [10] Peng Wang, Haitang Yang, and Shuxuan Ying. Thermodynamics and phase transition of a Gauss-Bonnet black hole in a cavity. *Phys. Rev. D*, 101(6):064045, 2020. [arXiv:1909.01275](https://arxiv.org/abs/1909.01275), [doi:10.1103/PhysRevD.101.064045](https://doi.org/10.1103/PhysRevD.101.064045).
- [11] Yuchen Huang, Hongmei Jing, Jun Tao, and Feiyu Yao. Phase structures and transitions of quintessence surrounding RN black holes in a grand canonical ensemble. *Chin. Phys. C*, 45(7):075101, 2021. [arXiv:2104.12617](https://arxiv.org/abs/2104.12617), [doi:10.1088/1674-1137/abf6c4](https://doi.org/10.1088/1674-1137/abf6c4).
- [12] Feiyu Yao. Scalarized Einstein–Maxwell-scalar black holes in a cavity. *Eur. Phys. J. C*, 81(11):1009, 2021. [arXiv:2107.12039](https://arxiv.org/abs/2107.12039), [doi:10.1140/epjc/s10052-021-09793-3](https://doi.org/10.1140/epjc/s10052-021-09793-3).
- [13] Yuchen Huang and Jun Tao. Thermodynamics and phase transition of BTZ black hole in a cavity. 12 2021. [arXiv:2112.13249](https://arxiv.org/abs/2112.13249).
- [14] Peng Wang, Houwen Wu, Haitang Yang, and Feiyu Yao. Extended Phase Space Thermodynamics for Black Holes in a Cavity. *JHEP*, 09:154, 2020. [arXiv:2006.14349](https://arxiv.org/abs/2006.14349), [doi:10.1007/JHEP09\(2020\)154](https://doi.org/10.1007/JHEP09(2020)154).
- [15] Peng Wang, Houwen Wu, and Haitang Yang. Thermodynamic Geometry of AdS Black Holes and Black Holes in a Cavity. *Eur. Phys. J. C*, 80(3):216, 2020. [arXiv:1910.07874](https://arxiv.org/abs/1910.07874), [doi:10.1140/epjc/s10052-020-7776-2](https://doi.org/10.1140/epjc/s10052-020-7776-2).
- [16] Peng Wang and Feiyu Yao. Thermodynamic geometry of black holes enclosed by a cavity in extended phase space. *Nucl. Phys. B*, 976:115715, 2022. [arXiv:2107.14640](https://arxiv.org/abs/2107.14640), [doi:10.1016/j.nuclphysb.2022.115715](https://doi.org/10.1016/j.nuclphysb.2022.115715).
- [17] Roy P. Kerr. Gravitational field of a spinning mass as an example of algebraically special metrics. *Phys. Rev. Lett.*, 11:237–238, 1963. [doi:10.1103/PhysRevLett.11.237](https://doi.org/10.1103/PhysRevLett.11.237).
- [18] E T. Newman, R. Couch, K. Chinnapared, A. Exton, A. Prakash, and R. Torrence. Metric of a Rotating, Charged Mass. *J. Math. Phys.*, 6:918–919, 1965. [doi:10.1063/1.1704351](https://doi.org/10.1063/1.1704351).
- [19] Juan Martin Maldacena. The Large N limit of superconformal field theories and supergravity. *Adv. Theor. Math. Phys.*, 2:231–252, 1998. [arXiv:hep-th/9711200](https://arxiv.org/abs/hep-th/9711200), [doi:10.1023/A:1026654312961](https://doi.org/10.1023/A:1026654312961).
- [20] Edward Witten. Anti-de Sitter space and holography. *Adv. Theor. Math. Phys.*, 2:253–291,

1998. [arXiv:hep-th/9802150](#), [doi:10.4310/ATMP.1998.v2.n2.a2](#).
- [21] Marco M. Caldarelli, Guido Cognola, and Dietmar Klemm. Thermodynamics of Kerr-Newman-AdS black holes and conformal field theories. *Class. Quant. Grav.*, 17:399–420, 2000. [arXiv:hep-th/9908022](#), [doi:10.1088/0264-9381/17/2/310](#).
- [22] P. C. W. Davies. Thermodynamic Phase Transitions of Kerr-Newman Black Holes in De Sitter Space. *Class. Quant. Grav.*, 6:1909, 1989. [doi:10.1088/0264-9381/6/12/018](#).
- [23] George Ruppeiner. Thermodynamic curvature and phase transitions in Kerr-Newman black holes. *Phys. Rev. D*, 78:024016, 2008. [arXiv:0802.1326](#), [doi:10.1103/PhysRevD.78.024016](#).
- [24] Anurag Sahay, Tapobrata Sarkar, and Gautam Sengupta. Thermodynamic Geometry and Phase Transitions in Kerr-Newman-AdS Black Holes. *JHEP*, 04:118, 2010. [arXiv:1002.2538](#), [doi:10.1007/JHEP04\(2010\)118](#).
- [25] J. A. R. Cembranos, A. de la Cruz-Dombriz, and P. Jimeno Romero. Kerr-Newman black holes in $f(R)$ theories. *Int. J. Geom. Meth. Mod. Phys.*, 11:1450001, 2014. [arXiv:1109.4519](#), [doi:10.1142/S0219887814500017](#).
- [26] A. Belhaj, M. Chabab, H. El Moumni, L. Medari, and M. B. Sedra. The Thermodynamical Behaviors of Kerr—Newman AdS Black Holes. *Chin. Phys. Lett.*, 30:090402, 2013. [arXiv:1307.7421](#), [doi:10.1088/0256-307X/30/9/090402](#).
- [27] Peng Cheng, Shao-Wen Wei, and Yu-Xiao Liu. Critical phenomena in the extended phase space of Kerr-Newman-AdS black holes. *Phys. Rev. D*, 94:024025, 2016. [arXiv:1603.08694](#), [doi:10.1103/PhysRevD.94.024025](#).
- [28] Tamás S. Biró, Viktor G. Czinner, Hideo Iguchi, and Péter Ván. Volume dependent extension of Kerr-Newman black hole thermodynamics. *Phys. Lett. B*, 803:135344, 2020. [arXiv:1912.04547](#), [doi:10.1016/j.physletb.2020.135344](#).
- [29] H. García-Compeán, V. S. Manko, and C. J. Ramírez-Valdez. Thermodynamics of two aligned Kerr-Newman black holes. *Phys. Rev. D*, 103(10):104001, 2021. [arXiv:2008.01213](#), [doi:10.1103/PhysRevD.103.104001](#).
- [30] Larry Smarr. Surface Geometry of Charged Rotating Black Holes. *Phys. Rev. D*, 7:289–295, 1973. [doi:10.1103/PhysRevD.7.289](#).
- [31] Erik A. Martinez. Quasilocal energy for a Kerr black hole. *Phys. Rev. D*, 50:4920–4928, 1994. [arXiv:gr-qc/9405033](#), [doi:10.1103/PhysRevD.50.4920](#).
- [32] Per Kraus, Finn Larsen, and Ruud Siebelink. The gravitational action in asymptotically

- AdS and flat space-times. *Nucl. Phys. B*, 563:259–278, 1999. [arXiv:hep-th/9906127](#), [doi:10.1016/S0550-3213\(99\)00549-0](#).
- [33] Robert B. Mann. Misner string entropy. *Phys. Rev. D*, 60:104047, 1999. [arXiv:hep-th/9903229](#), [doi:10.1103/PhysRevD.60.104047](#).
- [34] Vijay Balasubramanian and Per Kraus. A Stress tensor for Anti-de Sitter gravity. *Commun. Math. Phys.*, 208:413–428, 1999. [arXiv:hep-th/9902121](#), [doi:10.1007/s002200050764](#).
- [35] Stephen R. Lau. Light cone reference for total gravitational energy. *Phys. Rev. D*, 60:104034, 1999. [arXiv:gr-qc/9903038](#), [doi:10.1103/PhysRevD.60.104034](#).
- [36] M. H. Dehghani and Robert B. Mann. Quasilocal thermodynamics of Kerr and Kerr - anti-de Sitter space-times and the AdS / CFT correspondence. *Phys. Rev. D*, 64:044003, 2001. [arXiv:hep-th/0102001](#), [doi:10.1103/PhysRevD.64.044003](#).
- [37] M. H. Dehghani. Quasilocal thermodynamics of Kerr-de Sitter space-times and the AdS / CFT correspondence. *Phys. Rev. D*, 65:104030, 2002. [arXiv:hep-th/0201128](#), [doi:10.1103/PhysRevD.65.104030](#).
- [38] M. H. Dehghani and H. KhajehAzad. Thermodynamics of Kerr-Newman de Sitter black hole and dS / CFT correspondence. *Can. J. Phys.*, 81:1363, 2003. [arXiv:hep-th/0209203](#), [doi:10.1139/p03-110](#).
- [39] K. C. K. Chan, J. D. E. Creighton, and Robert B. Mann. Conserved masses in GHS Einstein and string black holes and consistent thermodynamics. *Phys. Rev. D*, 54:3892–3899, 1996. [arXiv:gr-qc/9604055](#), [doi:10.1103/PhysRevD.54.3892](#).
- [40] Eric Poisson. *A relativist's toolkit: the mathematics of black-hole mechanics*. Cambridge university press, 2004.
- [41] Laszlo B. Szabados. Quasi-Local Energy-Momentum and Angular Momentum in GR: A Review Article. *Living Rev. Rel.*, 7:4, 2004. [doi:10.12942/lrr-2004-4](#).